A Model-Independent Partial Wave Approach to Meson Photo- and Electroproduction

Spherical Harmonic Moments, Spin Density Matrices, Partial Wave Amplitudes

Derek Glazier
Dillon Leahy, Vincent Mathieu
and the Joint Physics Analysis Centre

EMMI RRTF Workshop – CERN, June 2026

Starting Point: CLAS 2009 $\pi^+\pi^-$ Moments Analysis

PRL **102,** 102001 (2009) PHYSICAL REVIEW LETTERS week ending 13 MARCH 2009

Measurement of Direct $f_0(980)$ Photoproduction on the Proton

M. Battaglieri,[1] R. De Vita,[1] A. P. Szczepaniak,[2] K. P. Adhikari,[34] M. Aghasyan,[19] M. J. Amaryan,[34] P. Ambrozewicz,[14] M. Anghinolfi,[1] G. Asryan,[47] H. Avakian,[41] H. Bagdasaryan,[34] N. Baillie,[46] J. P. Ball,[4] N. A. Baltzell,[40] V. Batourine,[26,41]

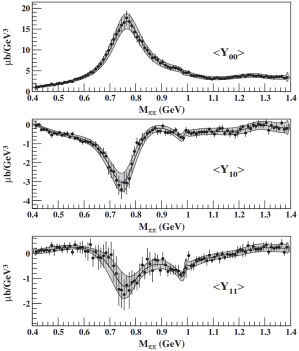

Fig A: *Extracted angular moments $\langle Y_{00}\rangle$, $\langle Y_{10}\rangle$, and $\langle Y_{11}\rangle$ mapping the clear S-P interference profiles.*

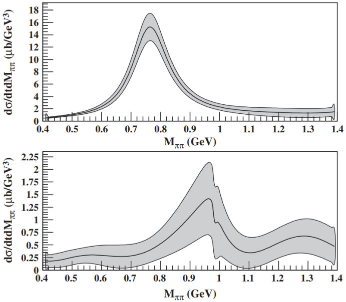

Fig B: *Resulting PWA cross sections cleanly splitting the small scalar S-wave from the dominant vector P-wave.*

Defining Angular Moments

$$\langle Y_{LM}\rangle = \sqrt{4\pi}\int d\Omega_\pi\, Y_{LM}\,\frac{d^3\sigma}{dt\, dM_{\pi\pi}\, d\Omega_\pi}$$

Disentangling *S* and *P* Waves

- **Overlap:** The $\pi^+\pi^-$ final state contains overlapping *S* and *P* wave amplitudes.
- **Scale Limit:** Direct scalar extraction is buried because the vector *P*-wave (ρ) cross section is $\sim 50\times$ larger.
- **Resolution:** Moments preserve the phase interference terms (e.g., $\langle Y_{10}\rangle$), allowing PWA to isolate the $f_0(980)$.
- model dependent due to unpolarised photon beam

Photoproduction Formalism: Intensity Decomposition & α Definition

Moments of angular distribution and beam asymmetries in $\eta\pi^0$ photoproduction at GlueX

V. Mathieu[1,2,*], M. Albaladejo[1,†], C. Fernández-Ramírez[3], A. W. Jackura[4,5], M. Mikhasenko[6], A. Pilloni[7,8], and A. P. Szczepaniak[1,4,5] (Joint Physics Analysis Center

The total differential cross section for two-spinless-meson photoproduction with an elliptically polarized photon beam splits into independent angular intensity components:

Total Intensity Decomposition

$$\mathcal{I}(\Omega, \Phi) = \mathcal{I}^0(\Omega) - P_L \mathcal{I}^1(\Omega)\cos(2\Phi) - P_L \mathcal{I}^2(\Omega)\sin(2\Phi) - P_C \mathcal{I}^3(\Omega)$$

Explicit Definition of the Beam Configuration Index α

The superscript $\alpha \in \{0, 1, 2, 3\}$ tracks the physical polarization operators acting on the photon density matrix :

Index α	Observable Component	Physical Beam State	Polarization Operator
$\alpha = 0$	$\mathcal{I}^0(\Omega)$	Unpolarized Beam Frame Baseline	Identity Matrix $\mathbf{1}$
$\alpha = 1$	$\mathcal{I}^1(\Omega)$	Linear Polarization ($\cos 2\Phi$ modulation)	Pauli Matrix σ_x
$\alpha = 2$	$\mathcal{I}^2(\Omega)$	Linear Polarization ($\sin 2\Phi$ modulation)	Pauli Matrix σ_y
$\alpha = 3$	$\mathcal{I}^3(\Omega)$	Circular Polarization Element	Pauli Matrix σ_z

Photoproduction Formalism: Reflectivity Amplitudes

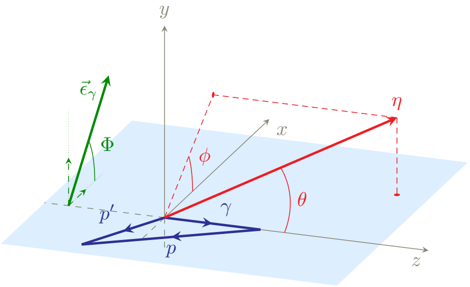

Figure: Gottfried-Jackson coordinate system configuration. The z-axis follows the incoming beam (γ), and the xz production plane contains the target (p) and recoil (p') nucleon trajectories .

Opposite reflectivities do not interfere and sum completely incoherently inside the observable matrix blocks, block-diagonalizing the parameter space .

To exploit parity conservation and isolate independent exchange naturalities, we transform the straight photon helicity production amplitudes $T_{\lambda_\gamma,m}$ into the reflectivity basis $[\ell]_m^{(\epsilon)}$:

Reflectivity Basis Definition

$$[\ell]_m^{(\epsilon)} = \frac{1}{\sqrt{2}} \left(T_{+1,m} - \epsilon(-1)^m T_{-1,-m} \right)$$

Physical Interpretation of Quantities

- **Reflectivity ($\epsilon = \pm 1$):** Characterizes reflection symmetry across the production plane. In the high-energy Regge limit, it cleanly separates exchanges of good naturality ($P = \epsilon(-1)^J$)
- **Meson Orbital Spin (ℓ):** Represents the total angular momentum J of the two-spinless-meson decay system.
- **Spin Projection (m) & Flips:** Tracks the meson spin projection along the quantization z-axis. The number of helicity flips is invariant between bases, : $\Delta\lambda = |m - \lambda_\gamma|$ for transverse photons.

Photoproduction Formalism: Spherical Harmonic Decomposition

Each distinct directional intensity component $\mathcal{I}^\alpha(\Omega)$ is expanded directly into orthogonal spherical harmonics to isolate the model-independent moments $H^\alpha(LM)$:

Spherical Harmonic Expansion

$$\mathcal{I}^\alpha(\Omega) = \kappa \sum_{L,M} H^\alpha(LM) Y_L^M(\Omega)$$

NOTE : These spherical harmonic moments summarize the most complete and general information that can be extracted from such an experiment.

Spin-Density Matrix Elements (SDMEs) to Partial Waves

The matrix elements are constructed as bilinear combinations of the underlying reflectivity partial-wave amplitudes $[\ell]_m^{(\epsilon)}$:

$$\rho^{0,\ell\ell'}_{mm'} = [\ell]_m^{(\epsilon)}[\ell']_{m'}^{(\epsilon)*} + (-1)^{m-m'}[\ell]_{-m}^{(\epsilon)}[\ell']_{-m'}^{(\epsilon)*}$$

$$\rho^{1,\ell\ell'}_{mm'} = -\epsilon\left((-1)^m[\ell']_{-m}^{(\epsilon)}[\ell]_{m'}^{(\epsilon)*} + (-1)^{m'}[\ell]_m^{(\epsilon)}[\ell']_{-m'}^{(\epsilon)*}\right)$$

$$\rho^{2,\ell\ell'}_{mm'} = -i\epsilon\left((-1)^m[\ell']_{-m}^{(\epsilon)}[\ell]_{m'}^{(\epsilon)*} - (-1)^{m'}[\ell]_m^{(\epsilon)}[\ell']_{-m'}^{(\epsilon)*}\right)$$

$$\rho^{3,\ell\ell'}_{mm'} = [\ell]_m^{(\epsilon)}[\ell']_{m'}^{(\epsilon)*} - (-1)^{m-m'}[\ell]_{-m}^{(\epsilon)}[\ell']_{-m'}^{(\epsilon)*}$$

Photoproduction Formalism: Classic Schilling & Wolf Projections

For an isolated pure vector state ($J = 1$, such as intermediate $\rho(770) \to \pi^+\pi^-$ decay), the explicit geometric angular expansions for the four beam configurations map strictly onto the classic SDME basis $\rho^{\alpha}_{mm'}$:

Truncated P-Wave Intensity Angular Projections

$$\mathcal{I}^0(\theta,\phi) = \frac{3}{4\pi}\left[\frac{1}{2}(1-\rho^0_{00}) + \frac{1}{2}(3\rho^0_{00}-1)\cos^2\theta - \sqrt{2}\,\mathrm{Re}[\rho^0_{10}]\sin 2\theta\cos\phi - \rho^0_{1-1}\sin^2\theta\cos 2\phi\right]$$

$$\mathcal{I}^1(\theta,\phi) = \frac{3}{4\pi}\left[\rho^1_{11}\sin^2\theta + \rho^1_{00}\cos^2\theta - \sqrt{2}\,\mathrm{Re}[\rho^1_{10}]\sin 2\theta\cos\phi - \rho^1_{1-1}\sin^2\theta\cos 2\phi\right]$$

$$\mathcal{I}^2(\theta,\phi) = \frac{3}{4\pi}\left[\sqrt{2}\,\mathrm{Im}[\rho^2_{10}]\sin 2\theta\sin\phi + \mathrm{Im}[\rho^2_{1-1}]\sin^2\theta\sin 2\phi\right]$$

$$\mathcal{I}^3(\theta,\phi) = \frac{3}{4\pi}\left[\sqrt{2}\,\mathrm{Im}[\rho^3_{10}]\sin 2\theta\sin\phi + \mathrm{Im}[\rho^3_{1-1}]\sin^2\theta\sin 2\phi\right]$$

Note: The angles θ and ϕ define the direction of the decay products inside the Gottfried-Jackson rest frame .

Photoproduction Formalism: Mapping Moments to Classic SDMEs

By performing explicit coordinate inversions of the orthogonal functions on Slide 2, we arrive at the exact algebraic dictionary linking experimental Moments $H^\alpha(LM)$ to the classic vector-meson SDMEs (when $H^0(0,0) \equiv 1$):

Classic SDMEs Extracted from Moments

$$\rho^0_{00} = \frac{1}{3}\left(5H^0(2,0) + 1\right)$$

$$\rho^0_{1-1} = -\frac{5}{\sqrt{6}} H^0(2,2)$$

$$\mathrm{Re}[\rho^0_{10}] = \frac{5}{\sqrt{12}} H^0(2,1)$$

$$\rho^1_{00} = -\frac{1}{3} H^1(0,0) - \frac{5}{3} H^1(2,0)$$

$$\rho^1_{11} = -\frac{1}{3} H^1(0,0) + \frac{5}{6} H^1(2,0)$$

$$\rho^1_{1-1} = \frac{5}{\sqrt{6}} H^1(2,2)$$

$$\mathrm{Re}[\rho^1_{10}] = -\frac{5}{\sqrt{12}} H^1(2,1)$$

$$\mathrm{Im}[\rho^2_{1-1}] = \frac{5}{\sqrt{6}} H^2(2,2)$$

$$\mathrm{Im}[\rho^2_{10}] = -\frac{5}{\sqrt{12}} H^2(2,1)$$

$$\mathrm{Im}[\rho^3_{1-1}] = \frac{5}{\sqrt{6}} H^3(2,2)$$

$$\mathrm{Im}[\rho^3_{10}] = -\frac{5}{\sqrt{12}} H^3(2,1)$$

Note: Spin-density matrix elements (SDMEs) as per the Diehl notation can be calculated directly from these Schilling and Wolf (S+W) SDMEs.

Electroproduction Formalism: 9-Component Intensity Expansion

When moving to virtual photons ($Q^2 > 0$), the introduction of longitudinal polarization expands the virtual-photon spin-density matrix into nine independent Hermitian response blocks ($\alpha = 0, \ldots, 8$):

Full Virtual Lepton-Hadron Angular Intensity

$\mathrm{I}(\Omega, \Phi) = I^0(\Omega) + \epsilon I^4(\Omega) - P_T I^1(\Omega) \cos 2\Phi - P_T I^2(\Omega) \sin 2\Phi + P_{T'} I^3(\Omega)$
$- \mathrm{P}_{LT} I^5(\Omega) \cos \Phi - P_{LT} I^6(\Omega) \sin \Phi + P_{LT'} I^7(\Omega) \cos \Phi + P_{LT'} I^8(\Omega) \sin \Phi$

General Formulation of the Observables

Each individual beam response component $I^\alpha(\Omega)$ expands directly into spherical harmonic moments $H^\alpha(LM)$ without truncation:

$$I^\alpha(\Omega) = s_\alpha \sum_{L,M} \sqrt{\frac{2L+1}{4\pi}} H^\alpha(LM) Y_L^M(\Omega) \quad \text{where} \quad s_\alpha = \begin{cases} 1 & \text{if } \alpha \in \{0, 4\} \\ -1 & \text{otherwise} \end{cases}$$

The moments map linearly to the underlying density matrix via fixed Clebsch-Gordan coefficients:

$$H^\alpha(LM) = s_\alpha \sum_{\ell, \ell', m, m'} \left(\frac{2\ell' + 1}{2\ell + 1} \right)^{1/2} C_{\ell 0 L 0}^{\ell' 0} C_{\ell m L M}^{\ell' m'} \rho_{mm'}^{\alpha, \ell\ell'}$$

Electroproduction Formalism: Virtual Photon Reflectivity Amplitudes

To maintain parity conservation and isolate independent exchange naturalities at $Q^2 > 0$, we separate the production amplitudes into Transverse (T) and Longitudinal (L) sectors within the reflectivity basis ($\epsilon = \pm 1$):

Reflectivity Amplitudes Formulation

$$[\ell]^{\epsilon}_{Tm} = \frac{1}{2}\left(T^{\ell}_{+1,m} - \epsilon(-1)^m T^{\ell}_{-1,-m}\right)$$

$$[\ell]^{\epsilon}_{Lm} = \frac{1}{2}\left(T^{\ell}_{0,m} + \epsilon(-1)^m T^{\ell}_{0,-m}\right)$$

Physical Definition of Amplitudes Quantum Numbers

- **Reflectivity ($\epsilon = \pm 1$):** Characterizes the reflection symmetry across the production plane to cleanly isolate exchange naturalities in the Regge limit. Opposite reflectivities sum completely incoherently within the observables.
- **Meson Orbital Spin (ℓ):** Dictates the total angular momentum J of the produced two-body meson decay system.
- **Spin Projection (m):** Quantifies the projection of the meson spin along the quantization z-axis inside the Gottfried-Jackson frame.

Electroproduction Formalism: Pure Transverse & Longitudinal Blocks

Operating in the general case without wave truncation, the diagonal photon response classes decompose directly into bilinear products of the reflectivity amplitudes $[\ell]^{\epsilon}_{X,m}$:

Pure Transverse Matrix Blocks ($\alpha = 0, 1, 2, 3$)

$$
\begin{aligned}
\rho^{0,\ell\ell'}_{mm'} &= \frac{\kappa}{2}\sum_{\epsilon}\Big([\ell]^{\epsilon}_{Tm}([\ell']^{\epsilon,*}_{Tm'}) + (-1)^{m'-m}[\ell]^{\epsilon}_{T,-m}([\ell']^{\epsilon,*}_{T,-m'})\Big)\\
\rho^{1,\ell\ell'}_{mm'} &= -\frac{\kappa}{2}\sum_{\epsilon}\epsilon\,\Big((-1)^{m}[\ell]^{\epsilon}_{T,-m}([\ell']^{\epsilon,*}_{Tm'}) + (-1)^{m'}[\ell]^{\epsilon}_{Tm}([\ell']^{\epsilon,*}_{T,-m'})\Big)\\
\rho^{2,\ell\ell'}_{mm'} &= -\frac{i\kappa}{2}\sum_{\epsilon}\epsilon\,\Big((-1)^{m}[\ell]^{\epsilon}_{T,-m}([\ell']^{\epsilon,*}_{Tm'}) - (-1)^{m'}[\ell]^{\epsilon}_{Tm}([\ell']^{\epsilon,*}_{T,-m'})\Big)\\
\rho^{3,\ell\ell'}_{mm'} &= \frac{\kappa}{2}\sum_{\epsilon}\Big([\ell]^{\epsilon}_{Tm}([\ell']^{\epsilon,*}_{Tm'}) - (-1)^{m'-m}[\ell]^{\epsilon}_{T,-m}([\ell']^{\epsilon,*}_{T,-m'})\Big)
\end{aligned}
$$

Pure Longitudinal Matrix Block ($\alpha = 4$)

$$
\rho^{4,\ell\ell'}_{mm'} = \kappa\sum_{\epsilon}[\ell]^{\epsilon}_{Lm}([\ell']^{\epsilon,*}_{Lm'})
$$

Note: The longitudinal response $\alpha = 4$ maps uniquely to longitudinal photon transitions ($[\ell]_L$). While the incoming virtual photon carries zero helicity ($\lambda_{\gamma^*} = 0$), the final hadronic states retain their full, un-truncated spin projections m and m'.

Electroproduction Formalism: Longitudinal-Transverse Interferences

The off-diagonal cross-talk terms represent interference blocks constructed from mixed products of Transverse (T) and Longitudinal (L) modes. They split cleanly into unpolarized and polarized electron beam sectors:

Unpolarized Lepton Beam Interferences ($\alpha = 5, 6$)

$$\rho^{5,\ell\ell'}_{mm'} = \frac{\kappa}{2\sqrt{2}} \sum_{\epsilon} \left([\ell]^{\epsilon}_{Lm}([\ell']^{-\epsilon,*}_{Tm'}) + [\ell]^{\epsilon}_{Tm}([\ell']^{-\epsilon,*}_{Lm'}) + (-1)^{m'-m} \left[[\ell]^{\epsilon}_{L,-m}([\ell']^{-\epsilon,*}_{T,-m'}) + [\ell]^{\epsilon}_{T,-m}([\ell']^{-\epsilon,*}_{L,-m'}) \right] \right)$$

$$\rho^{6,\ell\ell'}_{mm'} = -\frac{\kappa}{2\sqrt{2}} \sum_{\epsilon} \left([\ell]^{\epsilon}_{Lm}([\ell']^{-\epsilon,*}_{Tm'}) + [\ell]^{\epsilon}_{Tm}([\ell']^{-\epsilon,*}_{Lm'}) + (-1)^{m'-m} \left[[\ell]^{\epsilon}_{L,-m}([\ell']^{-\epsilon,*}_{T,-m'}) + [\ell]^{\epsilon}_{T,-m}([\ell']^{-\epsilon,*}_{L,-m'}) \right] \right)$$

Polarized Lepton Beam Interferences ($\alpha = 7, 8$)

$$\rho^{7,\ell\ell'}_{mm'} = \frac{\kappa}{2\sqrt{2}} \sum_{\epsilon} \left([\ell]^{\epsilon}_{Lm}([\ell']^{-\epsilon,*}_{Tm'}) + [\ell]^{\epsilon}_{Tm}([\ell']^{-\epsilon,*}_{Lm'}) - (-1)^{m'-m} \left[[\ell]^{\epsilon}_{L,-m}([\ell']^{-\epsilon,*}_{T,-m'}) + [\ell]^{\epsilon}_{T,-m}([\ell']^{-\epsilon,*}_{L,-m'}) \right] \right)$$

$$\rho^{8,\ell\ell'}_{mm'} = \frac{\kappa}{2\sqrt{2}} \sum_{\epsilon} \left([\ell]^{\epsilon}_{Lm}([\ell']^{-\epsilon,*}_{Tm'}) - [\ell]^{\epsilon}_{Tm}([\ell']^{-\epsilon,*}_{Lm'}) + (-1)^{m'-m} \left[[\ell]^{\epsilon}_{L,-m}([\ell']^{-\epsilon,*}_{T,-m'}) - [\ell]^{\epsilon}_{T,-m}([\ell']^{-\epsilon,*}_{L,-m'}) \right] \right)$$

Note: Amplitudes $[\ell]$ on the left inside the bilinear products track wave ℓ, while those on the right track wave ℓ'.

Relating Moments to Cross Sections

Experimentally, the purely transverse and longitudinal fluxes are combined unless separated via Rosenbluth techniques. One directly measures the photon polarization-weighted moment sum: $H^{04}(LM) = H^{0}(LM) + \epsilon H^{4}(LM)$.

Unpolarized 5-Fold Differential Cross Section

$$\frac{\mathrm{d}^5\sigma}{\mathrm{d}Q^2\,\mathrm{d}W\,\mathrm{d}t\,\mathrm{d}m\,\mathrm{d}\Phi} = \Gamma(Q^2, W)\left\{\frac{\mathrm{d}^2\sigma_T}{\mathrm{d}t\,\mathrm{d}m} + \epsilon\,\frac{\mathrm{d}^2\sigma_L}{\mathrm{d}t\,\mathrm{d}m} + \epsilon\cos(2\Phi)\,\frac{\mathrm{d}^2\sigma_{TT}}{\mathrm{d}t\,\mathrm{d}m}\right.$$
$$\left. + \sqrt{2\epsilon(1+\epsilon)}\cos(\Phi)\,\frac{\mathrm{d}^2\sigma_{LT}}{\mathrm{d}t\,\mathrm{d}m} + h_e\sqrt{2\epsilon(1-\epsilon)}\sin(\Phi)\,\frac{\mathrm{d}^2\sigma_{LT'}}{\mathrm{d}t\,\mathrm{d}m}\right\}$$

Parity Conservation & Missing Terms

Integrating over the solid angle $\mathrm{d}\Omega$ isolates the $L = 0, M = 0$ scalar moments: $\int I^{\alpha}(\Omega)\,\mathrm{d}\Omega = s_{\alpha} H^{\alpha}(00)$.

Result: For an unpolarized target and recoil ($\beta = \delta = 0$), parity dictates $S_{\alpha} = +1$. Responses with $S_{\alpha} = -1$ ($\alpha \in \{2, 3, 6, 7\}$) have analytically vanishing $M = 0$ states. Their associated imaginary cross-sections ($\sigma_{TT}^{\sin 2\Phi}, \sigma_{TT'}, \sigma_{LT}^{\sin\Phi}, \sigma_{LT'}^{\cos\Phi}$) are therefore strictly zero.

Mapping the Surviving Moments

$$\sigma_T = H^0(00) \qquad \sigma_L = H^4(00)$$
$$\sigma_{TT} = H^1(00) \qquad \sigma_{LT} = H^5(00)$$
$$\sigma_{LT'} = H^8(00)$$

Experimental Extraction and Normalization

Unbinned Extended Maximum Likelihood fits and other methods provide a set of *unscaled* relative moments, $\widehat{H}^{\alpha}(LM)$. To extract absolute cross sections, these fitted shapes must be scaled to the total experimental yield.

1. Fit Normalization Convention

We conventionally normalize the unscaled moments so the total unpolarized scalar component sums exactly to 2:

$$\widehat{H}^{04}(00) = \widehat{H}^{0}(00) + \epsilon \widehat{H}^{4}(00) = 2$$

2. Global Yield Constraint

The acceptance-corrected event yield in a kinematic bin ΔV is related to the integrated luminosity $\mathcal{L}$ and photon flux $\bar{\Gamma}$:

$$N_{\text{events}} = \mathcal{L} \cdot \Delta V \cdot \bar{\Gamma} \int_0^{2\pi} \mathrm{d}\Phi \int \mathrm{d}\Omega \, I(\Omega, \Phi)$$

Integrating out the azimuth Φ kills interference terms, isolating the true physical scalar moments:

3. The Absolute Scale Factor ($\mathcal{N}$)

Because true moments are proportional to fitted moments ($H^{\alpha} = \mathcal{N}\widehat{H}^{\alpha}$), substituting the fit convention yields the exact scale factor:

$$\mathcal{N} = \frac{N_{\text{events}}}{4\pi \cdot \mathcal{L} \cdot \Delta V \cdot \bar{\Gamma}}$$

Note: The 4π denominator arises naturally from the combination of the 2π azimuthal integral and the sum-to-2 fit convention.

4. Final Cross Section Extraction

Multiplying the extracted scalar moments by this kinematic scale factor yields the absolute differential cross sections isolated from the fit:

$$\frac{\mathrm{d}^2\sigma^{\alpha}}{\mathrm{d}t\,\mathrm{d}m} = \mathcal{N} \cdot \widehat{H}^{\alpha}(00)$$

Summary: Why Shift to the Reflectivity PWA Framework?

Transitioning from legacy density matrix parameters to an unconstrained reflectivity partial-wave analysis yields a substantial physics payoff at both vertices of the interaction:

1. Unraveling Hadronic Spectroscopy

- **Arbitrary Spin Extension:** Natively expands to accommodate arbitrary produced meson spins, moving past simple pure $J = 1$ vector truncations.
- **Disentangling Overlapping States:** Resolves and isolates states of different spins decaying simultaneously into the exact same final state channels.
- **Direct SDME Construction:** Provides an explicit algebraic formulation to calculate traditional Schilling-Wolf or Diehl SDMEs directly from the amplitudes.
- **Clean Parity Filtering:** Natively block-diagonalizes the equations, cleanly separating natural ($\epsilon = +1$) and unnatural ($\epsilon = -1$) exchange categories in the Regge picture.

2. Unlocking 3D Nucleon Structure

- **Strict Model Independence:** Reflectivity partial waves are model independent quantities, extracting clean observables free of hadronic production model assumptions.
- **Optimized L/T Separation:** Under t-channel Regge factorization no interference with top/bottom vertices. This isolates σ_L and σ_T from a single unpolarized energy dataset.
- **Polarised L/T Separation:** regain model independence when include polarised targets or recoil
- **Direct Translation to GPDs:** Isolated partial waves map directly to Compton Form Factors (CFFs), acting as exact quantum filters for the vector (H, E) and axial-vector $(\tilde{H}, \tilde{E})$ GPD families.

Moments to Partial Wave Amplitudes: The Inversion Procedure

Real Moments (H^0, H^1)

$$H^0(2,0) = \frac{2}{5}\sum_{\epsilon=\pm}\left(2|P_0^\epsilon|^2 - |P_{+1}^\epsilon|^2 - |P_{-1}^\epsilon|^2\right)$$

$$H^1(0,0) = 2\sum_{\epsilon=\pm}\epsilon\left(|P_0^\epsilon|^2 - 2|P_{+1}^\epsilon||P_{-1}^\epsilon|\cos\Delta\phi_{+1,-1}^\epsilon\right)$$

$$H^1(2,0) = \frac{4}{5}\sum_{\epsilon=\pm}\epsilon\left(|P_0^\epsilon|^2 + |P_{+1}^\epsilon||P_{-1}^\epsilon|\cos\Delta\phi_{+1,-1}^\epsilon\right)$$

$$H^0(2,1) = \frac{2\sqrt{3}}{5}\sum_{\epsilon=\pm}\left(|P_{+1}^\epsilon||P_0^\epsilon|\cos\Delta\phi_{+1,0}^\epsilon - |P_0^\epsilon||P_{-1}^\epsilon|\cos\Delta\phi_{0,-1}^\epsilon\right)$$

$$H^1(2,1) = \frac{2\sqrt{3}}{5}\sum_{\epsilon=\pm}\epsilon\left(|P_{+1}^\epsilon||P_0^\epsilon|\cos\Delta\phi_{+1,0}^\epsilon - |P_0^\epsilon||P_{-1}^\epsilon|\cos\Delta\phi_{0,-1}^\epsilon\right)$$

$$H^0(2,2) = -\frac{2\sqrt{6}}{5}\sum_{\epsilon=\pm}|P_{+1}^\epsilon||P_{-1}^\epsilon|\cos\Delta\phi_{+1,-1}^\epsilon$$

$$H^1(2,2) = \frac{\sqrt{6}}{5}\sum_{\epsilon=\pm}\epsilon\left(|P_{+1}^\epsilon|^2 + |P_{-1}^\epsilon|^2\right)$$

Note: We just show the example P-wave only. Similar sets of moments equations exist for all partial wave combinations.

Imaginary Moments (H^2, H^3)

$$H^2(2,1)/i = \frac{2\sqrt{3}}{5}\sum_{\epsilon=\pm}\epsilon\Big(-|P_{+1}^\epsilon||P_0^\epsilon|\cos\Delta\phi_{+1,0}^\epsilon - |P_0^\epsilon||P_{-1}^\epsilon|\cos\Delta\phi_{0,-1}^\epsilon\Big)$$

$$H^2(2,2)/i = \frac{\sqrt{6}}{5}\sum_{\epsilon=\pm}\epsilon\left(|P_{-1}^\epsilon|^2 - |P_{+1}^\epsilon|^2\right)$$

$$H^3(2,1)/i = \frac{2\sqrt{3}}{5}\sum_{\epsilon=\pm}\Big(|P_{+1}^\epsilon||P_0^\epsilon|\sin\Delta\phi_{+1,0}^\epsilon + |P_0^\epsilon||P_{-1}^\epsilon|\sin\Delta\phi_{0,-1}^\epsilon\Big)$$

$$H^3(2,2)/i = \frac{2\sqrt{6}}{5}\sum_{\epsilon=\pm}|P_{+1}^\epsilon||P_{-1}^\epsilon|\sin\Delta\phi_{+1,-1}^\epsilon$$

Numerical Inversion via MINUIT

The estimator matches experimental data against the partial-wave functional definitions:

$$\chi^2 = \sum_{\alpha,L,M}\frac{\left(H_{\rm exp}^\alpha(LM) - H_{\rm calc}^\alpha(LM)(\ell,m,\epsilon)\right)^2}{\sigma_{\alpha,LM}^2}$$

$\Longrightarrow$ **Amplitudes:** $|[\ell]_m^\epsilon|$ (Moduli tracker) **Phases:** ϕ_m^ϵ

Numerical Example: Photoproduction

Numerical inversion of the moment equations for an illustrative S and D-wave system demonstrates how increasing the polarization configuration (α) systematically eliminates mathematical degeneracies. We can determine the amplitudes as we have more observables (polarized moments) then real numbers from PW amplitudes.

1. Unpolarized (H^0)

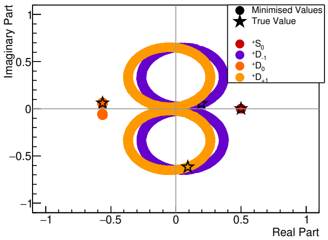

2. Linear (H^0, H^1, H^2)

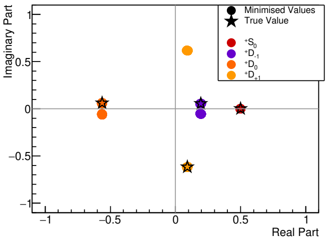

3. Elliptical (H^0, H^1, H^2, H^3)

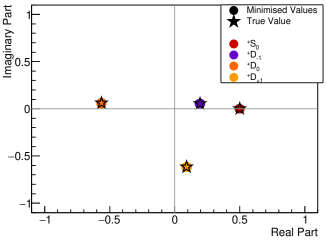

Continuous Ambiguity

The system of equations is under-constrained, resulting in an infinite family of valid solutions forming continuous bands.

Discrete Ambiguity

Linear observables provide enough constraints to collapse the continuous bands down to exactly **two discrete complex conjugate states** .

Unique Solution

Adding circular polarization (H^3) constrains the imaginary phase domains ($\sin \Delta\phi$), breaking the mirror symmetry to reveal a **single, unique solution**.

Numerical Example: Electroproduction (Transverse Sectors)

A fixed-amplitude closure study demonstrates the stability and uniqueness of the numerical inversion using a mock dataset generated up to D-waves ($\ell_{max} = 2$) :

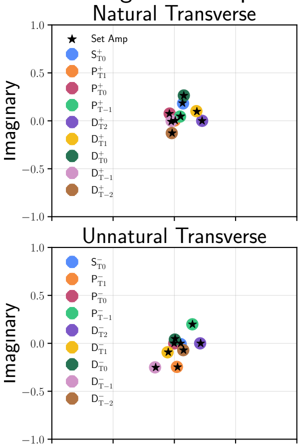

Full Parameter Space: Transverse sectors extracted cleanly.

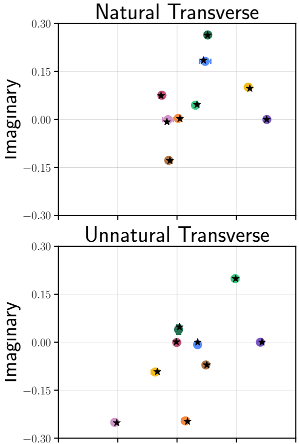

Zoomed Resolution Verification: Lack of false solution branches.

Numerical Example: Electroproduction (Longitudinal Sectors)

And the longitudinal sectors, where the fit basis remains highly overconstrained (31 equations for 20 parameters):

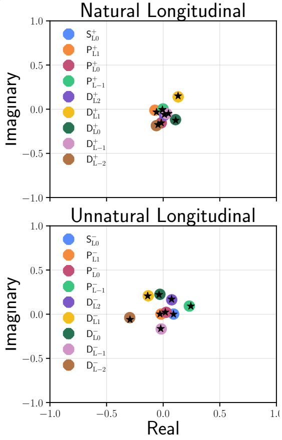

Full Parameter Space: Longitudinal sectors extracted cleanly.

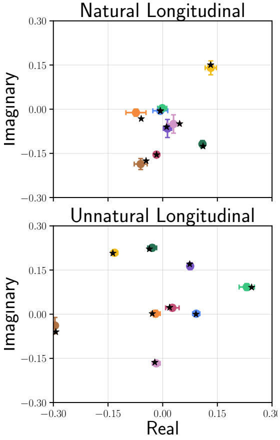

Zoomed Resolution Verification: High-resolution convergence space mapping.

Amplitude Level L/T Separation

- Traditional longitudinal-transverse (σ_L/σ_T) separation requires a Rosenbluth scan, necessitating costly beam energy changes.
- **Our Asumption:** By invoking t-channel **Regge Factorization**, the upper virtual-photon vertex factorizes cleanly from the lower nucleon vertex.

The Vertex Factorization Theorem

$$[l]^{\epsilon}_{cm;k}(Q^2, t, m) = \mathcal{V}^{c,\epsilon}_{\text{top}}(Q^2) \cdot \mathcal{D}_l(m) \cdot \mathcal{V}^{\epsilon}_{\text{bottom}}(t, k)$$

The Mathematical Extraction Advantage

Because the target-nucleon piece $\mathcal{V}^{\epsilon}_{\text{bottom}}$ carries **no dependence** on the photon's polarization state ($c \in \{T, L\}$), the relative phases of the target helicity sum are identical across the longitudinal and transverse sectors. Coherence is preserved in the LT interference terms, allowing an **extraction of partial wave amplitudes and thereby absolute σ_L and σ_T from a single unpolarized energy**.

Application to existing unpolarised target data

Spin density matrix elements in exclusive ρ^0 electroproduction on ^{1}H and ^{2}H targets at 27.5 GeV beam energy

Regular Article – Experimental Physics | Open access | Published: 17 July 2009
Volume 62, pages 659–695 (2009) Cite this article

Spin density matrix elements in exclusive ρ^0 meson muoproduction

Regular Article – Experimental Physics | Open access | Published: 13 October 2023
Volume 83, article number 924 (2023) Cite this article

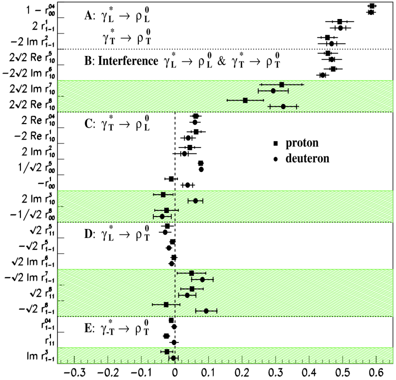

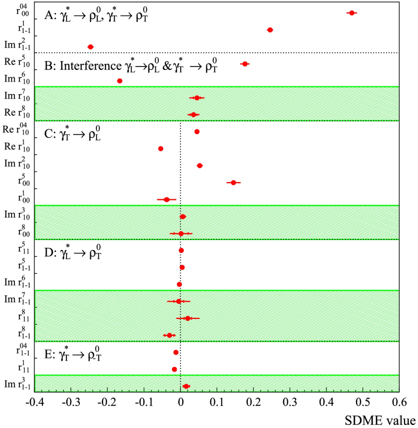

Real-World Data: ρ^0 Production (Transverse Sectors)

Applying the unconstrained reflectivity PWA numerical inversion to historical experimental data

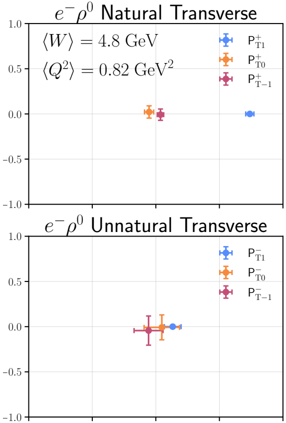

Electron Production: Extracted $e^-\rho^0$ transverse amplitudes .

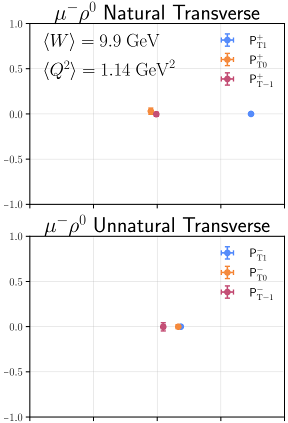

Muon Production: Extracted $\mu^-\rho^0$ transverse amplitudes.

Observation: Both independent datasets display structural agreement, dominated by a highly prominent Natural Transverse $m = 1$ no-helicity-flip amplitude ($[\ell]^+_{T1}$) signifying expected Pomeron/Reggeon exchange trajectories.

Real-World Data: ρ^0 Production (Longitudinal Sectors)

The corresponding longitudinal sector extractions illustrate clean isolation of the primary diffractive structures alongside structural symmetry constraints :

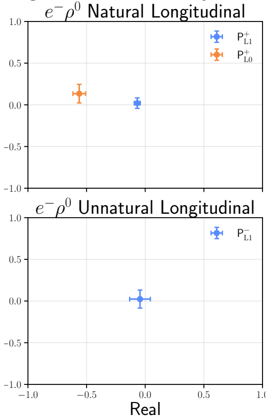

Electron Production: Extracted $e^-\rho^0$ longitudinal amplitudes.

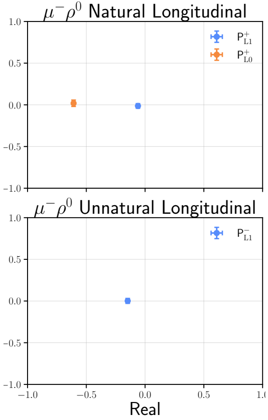

Muon Production: Extracted $\mu^-\rho^0$ longitudinal amplitudes.

Key Observation: The longitudinal sector shows clear dominance of the Natural Longitudinal $m = 0$ non-helicity-flip wave($[\ell]^+_{L0}$) which relates to twist 2 GPDs.

Experimental Results: Longitudinal-to-Transverse Ratio R

The extracted ratio of longitudinal to transverse cross sections, $R = \sigma_L/\sigma_T$ can now be calculated directly from the partial wave amplitudes

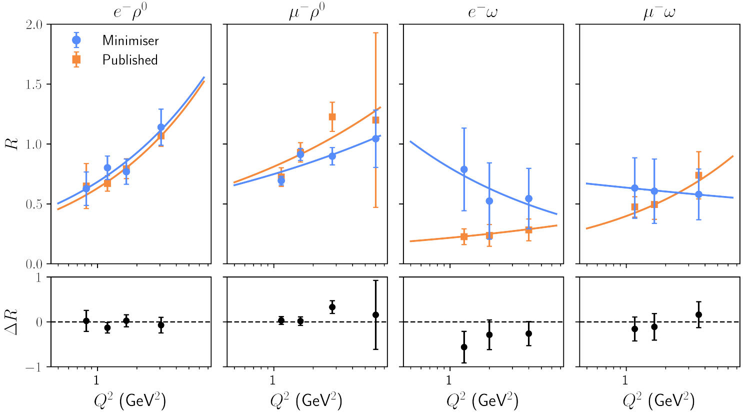

Direct Amplitude Derivation

R for ρ agrees well with published results, while for ω we see more significant differences due to contribution from unnatural pion pole term.

Complete Tensor Polarization: Accounting for Full Nucleon Spin

Intensity to amplitudes

1. **Global Angular Intensity (Measured Cross Section):**

$$I(\Omega, \Phi; \mathbf{S}_I, \mathbf{S}_R) = \sum_{\alpha=0}^{8} \sum_{\beta=0}^{3} \sum_{\delta=0}^{3} P_{\alpha\beta\delta}(\Phi, \mathbf{S}_I, \mathbf{S}_R)\, I^{\alpha\beta\delta}(\Omega)$$

2. **Decomposition into Component Intensities (Projected Moments):**

$$I^{\alpha\beta\delta}(\Omega) = s_{\alpha\beta\delta} \sum_{L,M} \sqrt{\frac{2L+1}{4\pi}}\, H^{\alpha\beta\delta}(LM)\, Y_L^M(\Omega)$$

3. **Extraction of Model-Independent Moments:** (Linear PWA)ace-0.25cm

$$H^{\alpha\beta\delta}(LM) = s_{\alpha\beta\delta} \sum_{\ell,\ell',m,m'} \left(\frac{2\ell'+1}{2\ell+1}\right)^{1/2} C_{\ell 0\, L0}^{\ell' 0}\, C_{\ell m\, LM}^{\ell' m'}\, \rho_{mm'}^{\alpha\beta\delta,\ell\ell'}$$

4. **Bilinear Production Amplitude Decomposition (Helicity Tensors):**

$$\rho_{mm'}^{\alpha\beta\delta,\ell\ell'} = \kappa \sum_{\Lambda} T^{\ell}_{\lambda m;\lambda_1\lambda_2}\, \Sigma^{\alpha}_{\lambda\lambda'}\, \sigma^{\beta}_{\lambda_1\lambda_1'}\, \sigma^{\delta}_{\lambda_2'\lambda_2}\, T^{\ell'*}_{\lambda' m';\lambda_1'\lambda_2'}$$

Polarisation Matrices

- $\boldsymbol{\alpha}$: Photon Matrix Σ^{α}
- $\boldsymbol{\beta}$: Initial Nucleon σ^{β}
- $\boldsymbol{\delta}$: Recoil Nucleon σ^{δ}

$$s_{\alpha\beta\delta} = \begin{cases} 1 & \alpha \in \{0,4\},\ \beta = \delta = 0 \\ -1 & \text{otherwise} \end{cases}$$

- $\boldsymbol{\Lambda} = \{\lambda, \lambda', \lambda_1, \lambda_1', \lambda_2, \lambda_2'\}$: Collective helicity indices
- λ, λ': Photon projection $(\pm 1, 0)$ · λ_1, λ_1': Initial nucleon
- λ_2, λ_2': Recoiling baryon
- $P_{\alpha\beta\delta}$: Combined polarisation direction
- Φ lepton/hadron plane
- S_I^{β} spin of initial proton
- S_R^{δ} spin of final baryon
- $\Omega = (\theta, \phi)$: Meson Decay angles

Electroproduction Formalism: Reduced Nucleon k-Basis

The virtual-photon parity relation allows us to collapse the four initial-recoil spin lines into just two independent sectors:

Parity Reduction to k-Basis

Using the common parity rule across photon sectors:

$$[\ell]^{\epsilon}_{Xm;-\lambda_1,-\lambda_2} = \epsilon(-1)^{\lambda_1-\lambda_2}[\ell]^{\epsilon}_{Xm;\lambda_1,\lambda_2}$$

We define two independent canonical states ($k \in \{-1,+1\}$):

$$\boldsymbol{k} = \mathbf{+1} \equiv [\ell]^{\epsilon}_{Xm;++} \quad \textbf{(Non-Flip)}$$
$$\boldsymbol{k} = \mathbf{-1} \equiv [\ell]^{\epsilon}_{Xm;+-} \quad \textbf{(Flip)}$$

The remaining states are fixed by parity completion:

$$[--] = \epsilon[+1], \qquad [-+] = -\epsilon[-1]$$

The Algebraic Advantage

- **Standard SDME Extraction:** Treats elements as independent variables, heavily inflating fit dimensionality.
- **PWA k-Basis Extraction:** Natively enforces parity, angular momentum.

The Over-Constrained Payoff: Vector Meson Truncation (P-wave only)

Kinematic Setup	Amps	Real Params	Moments/SDMEs	Physical Impact
Unpolarized	9	16	**23**	*Allows single-energy L/T separation*
Single-Polarized	18	35	**94**	*Also full seperation into k-amplitudes*
Double-Polarized	18	35	**376**	*Also full seperation into k-amplitudes*

Equivalence to Previous Work

In the limit we restrict our partial wave content to J=1, this formalism should be equivalent to previous amplitude formalisms

Vector meson production from a polarized nucleon

Markus Diehl

Published 17 September 2007 • Published under licence by IOP Publishing Ltd

Journal of High Energy Physics, Volume 2007, JHEP09(2007)

Citation Markus Diehl JHEP09(2007)064

DOI 10.1088/1126-6708/2007/09/064

Home › The European Physical Journal C › Article

Ratios of helicity amplitudes for exclusive ρ^0 electroproduction on transversely polarized protons

The HERMES Collaboration

Regular Article - Experimental Physics | Open access | Published: 08 June 2017

Volume 77, article number 378 (2017) Cite this article

New

Our formalism naturally extends to

- Any and mixed J (for spectroscopy)
- Polarised recoil (e.g. for $K^*\Lambda$)
- Defines moments as model independent data summary. (Up to some Lmax)
- Further extendable to final states other than 2 spin0 decay.

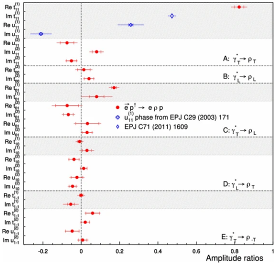

Modelling Vector Meson Production with Regge

PHYSICAL REVIEW D 97, 094003 (2018)

Vector meson photoproduction with a linearly polarized beam

V. Mathieu,[1,*] J. Nys,[1,2,3,4] C. Fernández-Ramírez,[5] A. Jackura,[3,4]
A. Pilloni,[1] N. Sherrill,[3,4] A. P. Szczepaniak,[1,3,4] and G. Fox[6]

(Joint Physics Analysis Center)

Regge Trajectory Classification

	Non-Flip ($k = +1$)	Spin-Flip ($k = -1$)
Natural ($\epsilon = +1$)	Pomeron ($\mathbb{P}$), f_2	a_2
Unnatural ($\epsilon = -1$)	f_1, a_1 (Neglected)	π, η (Pseudoscalar)

Core Modeling Principles

- **Vertex Factorization:** High-energy amplitudes factorize into independent photon (T^E) and nucleon (B^E) vertices linked by a Regge propagator $R^E(s, t)$.
- **Nucleon Constraints:** Isoscalar natural exchanges ($\mathbb{P}$, f_2) are empirically nucleon helicity non-flip, while the isovector a_2 dominates nucleon spin-flip currents.
- **Pseudoscalar Saturation:** Unnatural exchanges are saturated by active π and η trajectories, leaving charge-conjugation constraints to force a pure nucleon spin-flip structure.
- **Application:** Provides amplitude level calculations

Plan to refine with new GlueX data and extend to Q^2 with CLAS12 data.

SDME Grid

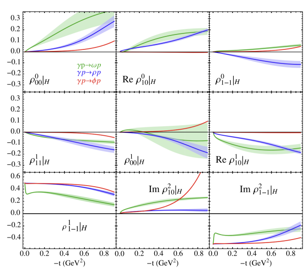

Cross Sections

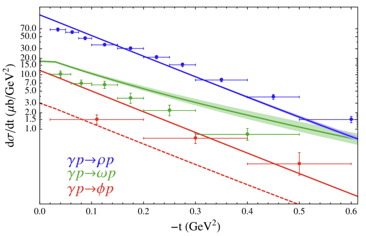

Electroproduction Event Generator : elSpectro - CLAS12/EIC

Virtual Photon Flux + Form Factor

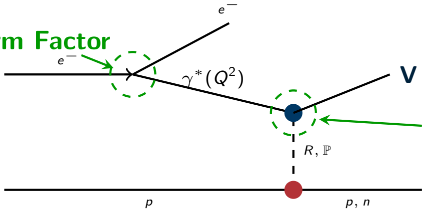

Photoproduction Amplitudes
→ from `jpacPhoto`
(Regge + VMD)

4-Fold Differential Cross Section Factorization

$$\frac{\mathrm{d}^4\sigma}{\mathrm{d}s\,\mathrm{d}Q^2\,\mathrm{d}\phi\,\mathrm{d}t} = \frac{\mathrm{d}^2\sigma_{e,\gamma^* e'}}{\mathrm{d}s\,\mathrm{d}Q^2} \times \frac{\mathrm{d}^2\sigma_{\gamma^*+p\to V+p}(s, Q^2)}{\mathrm{d}\phi\,\mathrm{d}t}$$

Kinematic Dictionary

$$L = \frac{1+(1-y)^2}{y} - \frac{2m_e^2 y}{Q^2}$$

$$K = \frac{W^2 - M^2}{2M} = \nu(1-x) = Ey(1-x) = \nu - \frac{Q^2}{2M}$$

Virtual Photon Flux Component

$$\frac{\mathrm{d}^2\sigma_{e,\gamma^* e'}}{\mathrm{d}s\,\mathrm{d}Q^2} = \frac{\alpha}{2\pi}\cdot\frac{K\cdot L}{E}\cdot\frac{1}{Q^2}\cdot\frac{1}{(s-M^2+Q^2)}$$

Physical Flux Trajectory

Photon flux rises rapidly as:

$$Q^2 \to 0 \quad ; \quad W = \sqrt{s} \to M_{\mathbf{proton}}$$

$\longrightarrow$ Drives highly elevated production rates.

Inclusive Vector Production Generator

Generator Pipeline Architecture

- **Hadronic Baseline:** Dynamically calculates transverse cross sections (σ_T) by wrapping the core JPAC Regge photoproduction model amplitudes.
- **Low-Q^2 Optimization:** Sets longitudinal components ($\sigma_L = 0$), providing a clean, high-speed framework tailored for quasi-real electroproduction tracking.
- **Flux Convolution:** Integrates the differential cross sections directly against the virtual photon flux to define total yields, sampling phase-space event generation proportionally.

Decay & Polarization Physics

- **Branching Channels:** Opens all native vector meson decay branches to track full multi-pion and kaon final-state kinematics.
- **Anisotropic Distributions:** Generates explicit decay angular topologies directly weighted by the calculated spin density matrix elements (SDMEs).

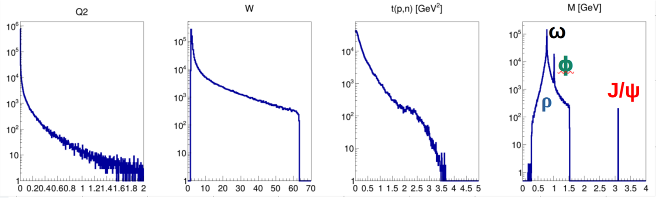

Generated inclusive production profiles tracking the clear ρ, ω, ϕ, and J/ψ mass states.

Generator Validation vs. `eStarlight` & `Pythia6` (ρ Production)

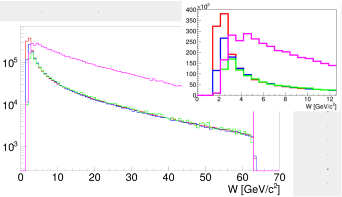

Q^2 Scaling Comparison

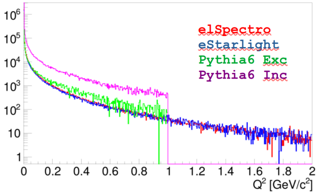

Hadronic Invariant Mass W

Summary and Outlook

Key Framework Objectives

- **Model Independence I:** Experimental data can be completely summarised by Polarised Spherical Harmonic moments $H^{\alpha}(LM)$.
- **Unpolarised Experiments:** Relating these moments to underlying partial wave amplitudes of any contributing meson resonances reduces number of independent parameters.
- **Polarised nucleons**: We generalised to polarised nucleons, doubling the measureable amplitudes.
- **L/T seperation** Restricting the model dependence to Regge factorisation allows Single Energy L/T seperations. In principle polarised nucleon experiments allow fully model indepedent extractions.

Current Status & Next Steps

- **Formalism:** paper write up in progress.
- **Tools:**
  - Moment to amplitude invertor developed.
  - Moment fitting tools for electro-production under-development.
  - Inclusive Generator based on JPAC models under-development.

Conclusion: Methods developed for complex amplitude analysis in photoproduction for Hadron Spectroscopy experiments are ready to be implemented in electro-production reactions.

Generalization to Polarized Target and Recoil

The macroscopic cross section expands systematically to include polarized initial targets ($\beta \in \{1, 2, 3\}$) and recoils ($\delta \in \{1, 2, 3\}$). We do not need a new normalization scheme; **the unpolarized scale factor ($\mathcal{N}$) anchors the entire polarized density matrix**.

Fully Polarized Macroscopic Cross Section

$$\frac{\mathrm{d}^5\sigma(\mathbf{S}_I, \mathbf{S}_R)}{\mathrm{d}Q^2\,\mathrm{d}W\,\mathrm{d}t\,\mathrm{d}m\,\mathrm{d}\Phi} = \Gamma(Q^2, W) \sum_{\alpha=0}^{8} \sum_{\beta=0}^{3} \sum_{\delta=0}^{3} P_{\alpha\beta\delta}(\Phi, \mathbf{S}_I, \mathbf{S}_R) \frac{\mathrm{d}^2\sigma^{\alpha\beta\delta}}{\mathrm{d}t\,\mathrm{d}m}$$

$$\text{Extraction Recipe:} \quad \sigma^{\alpha\beta\delta} = \mathcal{N} \cdot \widehat{H}^{\alpha\beta\delta}(00)$$

Activation of Imaginary Structure Functions (A_{UT}, A_{LL})

The imaginary interference responses ($\alpha \in \{2, 3, 6, 7\}$) strictly require a total parity product of $S_\alpha \tau_\beta \tau_\delta = +1$ to survive mathematically.

Case Study: Target Single-Spin Asymmetry ($A_{UT}^{\sin\Phi}$)
When an unpolarized beam ($\alpha = 6$, $S_6 = -1$) strikes a target polarized normal to the scattering plane ($\beta = 2$, $\tau_2 = -1$), the parity signs compensate:

$$(-1)_{S_\alpha} \times (-1)_{\tau_\beta} \times (+1)_{\tau_\delta} = +\mathbf{1}$$

This activates the scalar moment $H^{620}(00)$, producing the target SSA cross section:

$$\frac{\mathrm{d}^2\sigma_{LT}^{\sin\Phi, y}}{\mathrm{d}t\,\mathrm{d}m} = \mathcal{N} \cdot \widehat{H}^{620}(00)$$

The k-basis formalism mathematically mandates which observables require nucleon polarization to become experimentally accessible.

SDM Topology: Initial–Recoil Polarization Mapping

Pick a polarised experiment :

Recoil Polarization Index (δ)

Initial Polarization Index (β)

	0 (U)	1 (x)	2 (y)	3 (z)
0 (U)	$0,0$	$0,1$	$0,2$	$0,3$
1 (x)	$1,0$	$1,1$	$1,2$	$1,3$
2 (y)	$2,0$	$2,1$	$2,2$	$2,3$
3 (z)	$3,0$	$3,1$	$3,2$	$3,3$

SDM Topology Classes:

- $\epsilon' = \epsilon, k' = k$ (Fully Diagonal)
- $\epsilon' = \epsilon, k' = -k$ (Refl. Preserved)
- $\epsilon' = -\epsilon, k' = k$ (Helicity Preserved)
- $\epsilon' = -\epsilon, k' = -k$ (Fully Off-Diag.)

Note: $\beta + \delta$ = even (Blue/Green) isolates block-diagonal reflectivity elements; $\beta + \delta$ = odd (Yellow/Red) isolates the naturality-interference cross-terms.

Spin Density Matrix: Interference Projections

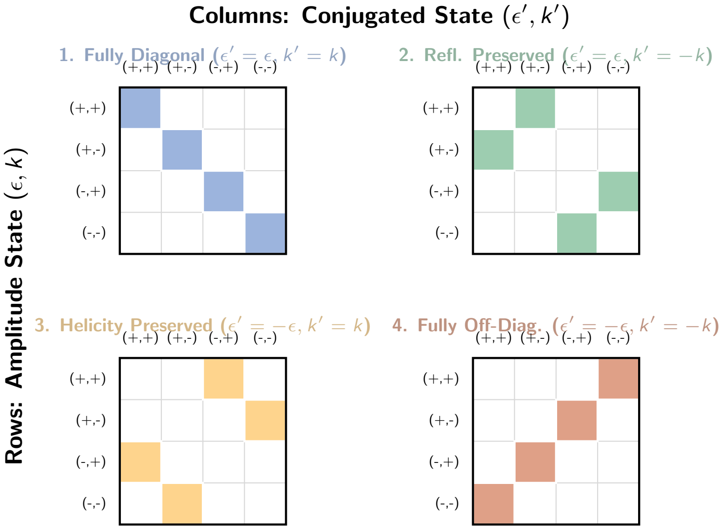

- **Diagonal Classes (1, 2):** Map intensities and nucleon-spin interference within fixed exchange naturalities.
- **Off-Diagonal Classes (3, 4):** Isolate interference between Natural and Unnatural exchange parities.

Inside the (ϵ, k) Matrix

By zooming in on the 4×4 matrix, we can see exactly how the exchange naturality (ϵ) and the nucleon helicity (k) map to specific physical interference terms.

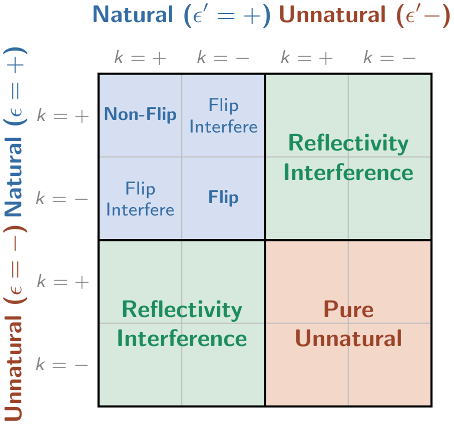

General Sub-Matrix Dimensions

Each cell represents an interference block of amplitudes $[\ell]^{\epsilon}_{Xm;k}$. The number of elements inside each block depends on the allowed partial waves (ℓ, m) and photon states $(X \in \{L, T\})$.

- **Natural Amps (N^+):** Contains all allowed Transverse and Longitudinal partial waves.
- **Unnatural Amps (N^-):** Contains strictly fewer states than N^+, because the unnatural Longitudinal $L_{m=0}$ state vanishes analytically due to parity conservation.

Case Study: Vector Meson $(\ell = 1)$

For a vector meson, the 9 partial waves per k-sector split asymmetrically:

- **Natural $(N^+ = 5)$:** $T_1, T_0, T_{-1}, L_1, L_0$
- **Unnatural $(N^- = 4)$:** T_1, T_0, T_{-1}, L_1

Consequently, the intersecting cells form heterogeneously sized matrices:

- **Pure Natural:** $N^+ \times N^+ = \mathbf{5} \times \mathbf{5}$ sub-matrix
- **Parity Interf.:** $N^+ \times N^- = \mathbf{5} \times \mathbf{4}$ sub-matrix
- **Pure Unnatural:** $N^- \times N^- = \mathbf{4} \times \mathbf{4}$ sub-matrix

Electroproduction Formalism VII: Polarized Target and Recoil

Activating initial target ($\beta > 0$) or final recoil ($\delta > 0$) polarization breaks the k-degeneracy. The Pauli spin matrices ($\sigma^\beta, \sigma^\delta$) act as mathematical operators, explicitly coupling the nucleon helicity transitions (k' and k):

Generalized Polarized Response Blocks

Pure Transverse Example ($\alpha = 0$):

$$\rho^{0\beta\delta}_{mm'} = \frac{\kappa}{2} \sum_{k',k,\epsilon} \langle k'|\sigma^\beta \sigma^\delta|k\rangle \Big([\ell]^{\epsilon}_{\mathrm{T}m;k'} [\ell']^{\epsilon *}_{\mathrm{T}m';k} + (-1)^{m'-m} [\ell]^{\epsilon}_{\mathrm{T},-m;k'} [\ell']^{\epsilon *}_{\mathrm{T},-m';k} \Big)$$

Pure Longitudinal Example ($\alpha = 4$):

$$\rho^{4\beta\delta}_{mm'} = \kappa \sum_{k',k,\epsilon} \langle k'|\sigma^\beta \sigma^\delta|k\rangle \Big([\ell]^{\epsilon}_{\mathrm{L}m;k'} [\ell']^{\epsilon *}_{\mathrm{L}m';k} \Big)$$

Longitudinal-Transverse Example ($\alpha = 5$):

$$\rho^{5\beta\delta}_{mm'} = \frac{\kappa}{2\sqrt{2}} \sum_{k',k,\epsilon} \langle k'|\sigma^\beta \sigma^\delta|k\rangle \Big([\ell]^{\epsilon}_{\mathrm{L}m;k'} [\ell']^{-\epsilon *}_{\mathrm{T}m';k} + [\ell]^{\epsilon}_{\mathrm{T}m;k'} [\ell']^{-\epsilon *}_{\mathrm{L}m';k} \pm \dots \Big)$$

The Spin Filter: Isolating the Physics

The operator $\langle k'|\sigma^\beta\sigma^\delta|k\rangle$ acts as a strict selector switch for the interference topologies.

1. Unpolarized ($\beta = 0, \delta = 0$): $\sigma^0 = \mathbb{I}$
Forces $k' = k$. The sums collapse to $\sum_k A_k A_k^*$. Non-flip and flip transitions cannot interfere.

2. Transverse Target ($\beta = 2$): $\sigma^2 = \sigma_y$
The Pauli-y matrix is off-diagonal. It strictly forces $k' = -k$. The response entirely isolates the interference between nucleon non-flip ($k = +1$) and spin-flip ($k = -1$) amplitudes.

3. Longitudinal Target ($\beta = 3$): $\sigma^3 = \sigma_z$
The Pauli-z matrix is diagonal. It forces $k' = k$ but applies a relative sign difference ($+1$ for $k = +1$, -1 for $k = -1$).

Phenomenological Rule: *Target/Recoil polarization does not alter the photon reflectivity (ϵ) couplings; it exclusively unlocks the hidden nucleon helicity (k) interferences.*

Electroproduction Formalism: The 9 Response Categories

Expanding the unpolarized system in this reduced k-basis explicitly isolates the 9 independent virtual-photon response blocks from same-reflectivity bilinears. Structures are identical for $\beta, \delta \neq 0$:

Pure Transverse Response Blocks ($\alpha = 0, 1, 2, 3$)

$$\rho^{0,\ell\ell'}_{mm'} = \frac{\kappa}{2} \sum_{k,\epsilon} \left([\ell]^{\epsilon}_{\mathrm{T}m;k} [\ell']^{\epsilon *}_{\mathrm{T}m';k} + (-1)^{m'-m} [\ell]^{\epsilon}_{\mathrm{T},-m;k} [\ell']^{\epsilon *}_{\mathrm{T},-m';k} \right)$$

$$\rho^{1,\ell\ell'}_{mm'} = -\frac{\kappa}{2} \sum_{k,\epsilon} \epsilon \left((-1)^{m} [\ell]^{\epsilon}_{\mathrm{T},-m;k} [\ell']^{\epsilon *}_{\mathrm{T}m';k} + (-1)^{m'} [\ell]^{\epsilon}_{\mathrm{T}m;k} [\ell']^{\epsilon *}_{\mathrm{T},-m';k} \right)$$

$$\rho^{2,\ell\ell'}_{mm'} = -\frac{i\kappa}{2} \sum_{k,\epsilon} \epsilon \left((-1)^{m} [\ell]^{\epsilon}_{\mathrm{T},-m;k} [\ell']^{\epsilon *}_{\mathrm{T}m';k} - (-1)^{m'} [\ell]^{\epsilon}_{\mathrm{T}m;k} [\ell']^{\epsilon *}_{\mathrm{T},-m';k} \right)$$

$$\rho^{3,\ell\ell'}_{mm'} = \frac{\kappa}{2} \sum_{k,\epsilon} \left([\ell]^{\epsilon}_{\mathrm{T}m;k} [\ell']^{\epsilon *}_{\mathrm{T}m';k} - (-1)^{m'-m} [\ell]^{\epsilon}_{\mathrm{T},-m;k} [\ell']^{\epsilon *}_{\mathrm{T},-m';k} \right)$$

Pure Longitudinal Response Block ($\alpha = 4$)

$$\rho^{4,\ell\ell'}_{mm'} = \kappa \sum_{k,\epsilon} [\ell]^{\epsilon}_{\mathrm{L}m;k} [\ell']^{\epsilon *}_{\mathrm{L}m';k}$$

Longitudinal-Transverse Interferences ($\alpha = 5, 6, 7, 8$)

$$\begin{aligned} \rho^{5,\ell\ell'}_{mm'} = \frac{\kappa}{2\sqrt{2}} \sum_{k,\epsilon} \Big(& [\ell]^{\epsilon}_{\mathrm{L}m;k} [\ell']^{-\epsilon *}_{\mathrm{T}m';k} + [\ell]^{\epsilon}_{\mathrm{T}m;k} [\ell']^{-\epsilon *}_{\mathrm{L}m';k} \\ & + (-1)^{m'-m} \left([\ell]^{\epsilon}_{\mathrm{L},-m;k} [\ell']^{-\epsilon *}_{\mathrm{T},-m';k} + [\ell]^{\epsilon}_{\mathrm{T},-m;k} [\ell']^{-\epsilon *}_{\mathrm{L},-m';k} \right) \Big) \end{aligned}$$

$$\begin{aligned} \rho^{6,\ell\ell'}_{mm'} = -\frac{\kappa}{2\sqrt{2}} \sum_{k,\epsilon} \Big(& [\ell]^{\epsilon}_{\mathrm{L}m;k} [\ell']^{-\epsilon *}_{\mathrm{T}m';k} + [\ell]^{\epsilon}_{\mathrm{T}m;k} [\ell']^{-\epsilon *}_{\mathrm{L}m';k} \\ & + (-1)^{m'-m} \left([\ell]^{\epsilon}_{\mathrm{L},-m;k} [\ell']^{-\epsilon *}_{\mathrm{T},-m';k} + [\ell]^{\epsilon}_{\mathrm{T},-m;k} [\ell']^{-\epsilon *}_{\mathrm{L},-m';k} \right) \Big) \end{aligned}$$

$$\begin{aligned} \rho^{7,\ell\ell'}_{mm'} = \frac{\kappa}{2\sqrt{2}} \sum_{k,\epsilon} \Big(& [\ell]^{\epsilon}_{\mathrm{L}m;k} [\ell']^{-\epsilon *}_{\mathrm{T}m';k} + [\ell]^{\epsilon}_{\mathrm{T}m;k} [\ell']^{-\epsilon *}_{\mathrm{L}m';k} \\ & - (-1)^{m'-m} \left([\ell]^{\epsilon}_{\mathrm{L},-m;k} [\ell']^{-\epsilon *}_{\mathrm{T},-m';k} + [\ell]^{\epsilon}_{\mathrm{T},-m;k} [\ell']^{-\epsilon *}_{\mathrm{L},-m';k} \right) \Big) \end{aligned}$$

$$\begin{aligned} \rho^{8,\ell\ell'}_{mm'} = \frac{\kappa}{2\sqrt{2}} \sum_{k,\epsilon} \Big(& [\ell]^{\epsilon}_{\mathrm{L}m;k} [\ell']^{-\epsilon *}_{\mathrm{T}m';k} - [\ell]^{\epsilon}_{\mathrm{T}m;k} [\ell']^{-\epsilon *}_{\mathrm{L}m';k} \\ & + (-1)^{m'-m} \left([\ell]^{\epsilon}_{\mathrm{L},-m;k} [\ell']^{-\epsilon *}_{\mathrm{T},-m';k} - [\ell]^{\epsilon}_{\mathrm{T},-m;k} [\ell']^{-\epsilon *}_{\mathrm{L},-m';k} \right) \Big) \end{aligned}$$

Symmetry Rule: *Pure T and L blocks sum over identical reflectivities (ϵ), while cross-talk LT components step anti-diagonally via ($\epsilon \cdot -\epsilon$)*